# Tesla Coil Impedance

Dr. Gary L. Johnson
Professor Emeritus
Electrical and Computer Engineering Department
Kansas State University
gjohnson@ksu.edu

## Abstract

*The input impedance of a Tesla coil operated as an 'extra' coil, or as a quarter-wave antenna above a ground plane, is given here. Effects of coil form, wire size, wire insulation, and humidity are discussed.*

## 1. Introduction

A classical Tesla coil contains two stages of voltage increase. The first is a conventional iron core transformer that steps up the available line voltage to a voltage in the range of 12 to 50 kV, 60 Hz. The second is a resonant air core transformer (the Tesla coil itself) which steps up the voltage to the range of 200 kV to 1 MV. The high voltage output is at a frequency much higher than 60 Hz, perhaps 500 kHz for the small units and 80 kHz (or less) for the very large units.

The lumped circuit model for the classical Tesla coil is shown in Fig. 1. The primary capacitor $C_1$ is a low loss ac capacitor, rated at perhaps 20 kV, and often made from mica or polyethylene. The primary coil $L_1$ is usually made of 4 to 15 turns for the small coils and 1 to 5 turns for the large coils. The secondary coil $L_2$ consists of perhaps 50 to 400 turns for the large coils and as many as 400 to 1000 turns for the small coils. The secondary capacitance $C_2$ is not a discrete commercial capacitor but rather is the distributed capacitance between the windings of $L_2$ and the voltage grading structure at the top of the coil (a toroid or sphere) and ground. This capacitance changes with the volume charge density around the secondary, increasing somewhat when the sparks start. It also changes with the surroundings of the coil, increasing as the coil is moved closer to a metal wall.

The symbol $G$ represents a spark gap, a device which will arc over at a sufficiently high voltage. The simplest version is just two metal spheres in air, separated by a small air gap. It acts as a voltage controlled switch in this circuit. The open circuit impedance of the gap is
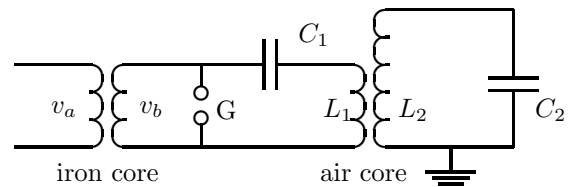


Figure 1: The Classical Tesla Coil

very high. The impedance during conduction depends on the geometry of the gap and the type of gas (usually air), and is a nonlinear function of the current density. This impedance is not negligible. A considerable fraction of the total input power goes into the production of light, heat, and chemical products at the spark gap.

The arc in the spark gap is similar to that of an electric arc welder in visual intensity. That is, one should not stare at the arc because of possible damage to the eyes. At most displays of classical Tesla coils, the spark gap makes more noise and produces more light than the electrical display at the top of the coil.

When the gap is not conducting, the capacitor $C_1$ is being charged in the circuit shown in Fig. 2, where just the central part of Fig. 1 is shown. The inductive reactance is much smaller than the capacitive reactance at 60 Hz, so $L_1$ appears as a short at 60 Hz and the capacitor is being charged by the iron core transformer secondary.

A common type of iron core transformer used for small Tesla coils is the neon sign transformer (NST). Secondary ratings are typically 9, 12, or 15 kV and 30 or 60 mA. An NST has a large number of turns on the secondary and a very high inductance. This inductance will limit the current into a short circuit at about the rated value. An operating neon sign has a low impedance, so current limiting is important to long
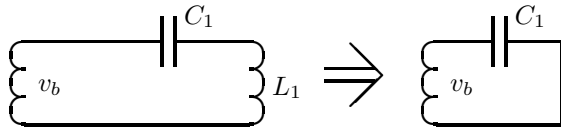
Figure 2: $C_1$ Being Charged With The Gap Open

transformer life. However, in Tesla coil use, the NST inductance will resonate with $C_1$. The NST may supply two or three times its rated current in this application. Overloading the NST produces longer sparks, but may also cause premature failure.

When the voltage across the capacitor and gap reaches a given value, the gap arcs over, resulting in the circuit in Fig. 3. We are not interested in efficiency in this introduction so we will model the arc as a short circuit. The shorted gap splits the circuit into two halves, with the iron core transformer operating at 60 Hz and the circuit to the right of the gap operating at a frequency (or frequencies) determined by $C_1$, $L_1$, $L_2$, and $C_2$. It should be noted that the output voltage of the iron core transformer drops to (approximately) zero while the input voltage remains the same, as long as the arc exists. The current through the transformer is limited by the transformer equivalent series impedance shown as $R_s + jX_s$ in Fig. 3. As mentioned, this operating mode is not a problem for the NST. However, the large Tesla coils use conventional transformers with per unit impedances in the range of 0.05 to 0.1. A transformer with a per unit impedance of 0.1 will experience a current of ten times rated while the output is shorted. Most transformers do not survive very long under such conditions. The solution is to include additional reactance in the input circuit.
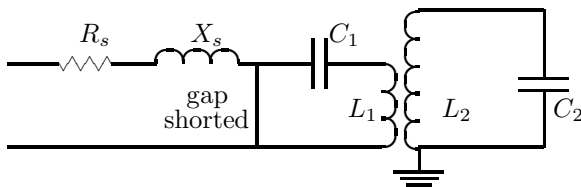


Figure 3: Tesla Circuit With Gap Shorted.

The equivalent lumped circuit model of the Tesla coil while the gap is shorted is shown in Fig. 4. $R_1$ and $R_2$ are the effective resistances of the air cored transformer primary and secondary, respectively. The mutual inductance between the primary and secondary is shown

by the symbol $M$. The coefficient of coupling is well under unity for an air cored transformer, so the ideal transformer model used for an iron cored transformer that electrical engineering students study in the first course on energy conversion does not apply here.
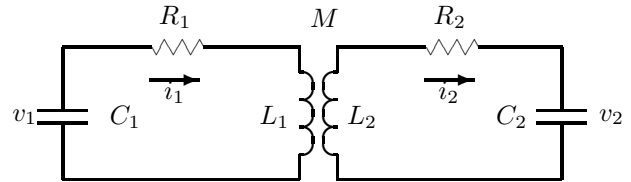


Figure 4: Lumped Circuit Model Of A Tesla Coil, arc on.

At the time the gap arcs over, all the energy is stored in $C_1$. As time increases, energy is shared among $C_1$, $L_1$, $C_2$, $L_2$, and $M$. The total energy in the circuit decreases with time because of losses in the resistances $R_1$ and $R_2$. There are four energy storage devices so a fourth order differential equation must be solved. The initial conditions are some initial voltage $v_1$, and $i_1 = i_2 = v_2 = 0$. If the arc starts again before all the energy from the previous arc has been dissipated, then the initial conditions must be changed appropriately.

With proper design (proper values of $C_1$, $L_1$, $C_2$, $L_2$, and $M$) it is possible to have all the energy in $C_1$ transferred to the secondary at some time $t_1$. That is, at $t_1$ there is no voltage across $C_1$ and no current through $L_1$. If the gap can be opened at $t_1$, then there is no way for energy to get back into the primary. No current can flow, so no energy can be stored in $L_1$, and without current the capacitor cannot be charged. The secondary then becomes a separate RLC circuit with nonzero initial conditions for both $C_2$ and $L_2$, as shown in Fig. 5. This circuit will then oscillate or "ring" at a resonant frequency determined by $C_2$ and $L_2$. With the gap open, the Tesla coil secondary is simply an RLC circuit, described in any text on circuit theory. The output voltage is a damped sinusoid.
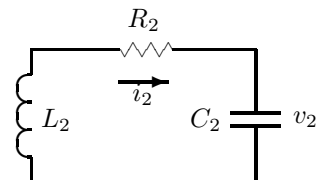


Figure 5: Lumped Circuit Model Of A Tesla Coil, arc off.

Finding a peak value for $v_2$ given some initial value for $v_1$ thus requires a two step solution process. We first solve a fourth order differential equation to find $i_2$ and $v_2$ as a function of time. At some time $t_1$ the circuit changes to the one shown in Fig. 5, which is described by a second order differential equation. The initial conditions are the values of $i_2$ and $v_2$ determined from the previous solution at time $t_1$. The resulting solution then gives the desired peak values for voltage and current. The process is tedious, but can readily be done on a computer. It yields some good insights as to the effects of parameter variation. It helps establish a benchmark for optimum performance and also helps identify parameter values that are at least of the correct order of magnitude. However, there are several limitations to the process which must be kept in mind.

First, the arc is very difficult to characterize accurately in this model. The equivalent $R_1$ will change, perhaps by an order of magnitude, with factors like $i_1$, ambient humidity, and the condition, geometry, and temperature of the electrode materials. This introduces a very significant error into the results.

Second, the arc is not readily turned off at a precise instant of time. The space between electrodes must be cleared of the hot conducting plasma (the current carrying ions and electrons) before the spark gap can return to its open circuit mode. Otherwise, when energy starts to bounce back from the secondary, a voltage will appear across the spark gap, and current will start to flow again, after the optimum time $t_1$ has passed. With fixed electrodes, the plasma is dissipated by thermal and chemical processes that require tens of microseconds to function. When we consider that the optimum $t_1$ may be 2 $\mu$s, a problem is obvious. This dissipation time can be decreased significantly by putting a fan on the electrodes to blow the plasma away. This also has the benefit of cooling the electrodes. For more powerful systems, however, the most common method is a rotating spark gap. A circular disc with several electrodes mounted on it is driven by a motor. An arc is established when a moving electrode passes by a stationary electrode, but the arc is immediately stretched out by the movement of the disc. During the time around a current zero, the resistance of the arc can increase to where the arc cannot be reestablished by the following increase in voltage.

The rotary spark gap still has limitations on the minimum arc time. Suppose we consider a disc with a radius of 0.2 m and a rotational speed of 400 rad/sec (slightly above 3600 RPM). The edge of the disc is moving at a linear velocity of $r\omega = 80$ m/s. Suppose also that an arc cannot be sustained with arc lengths above 2 cm. It requires $0.02/80 = 25$ $\mu$s for the disc to turn this distance. This time can be shortened by making the disc larger or by turning it at a higher rate of speed, but in both cases we worry about the stress limits of the disc. Nobody wants fragments of a failed disc flying around the room. The practical lower limit of arc length seems to be about 10 $\mu$s. With larger coils this may be reasonably close to the optimum value.

The third reason for concern about the above calculations is that the Tesla coil secondary has features that cannot be precisely modeled by a lumped circuit. One such feature is ringing at 'harmonic' frequencies. Neither distributed nor lumped models do a particularly good job of predicting these frequencies. For example, a medium sized secondary might usually ring down at 160 kHz. Sometimes, however, it will ring down at $3.5(160) = 560$ kHz. A third harmonic appears in many electrical circuits and has plausible explanations. A 3.5 'harmonic' is another story entirely.

## 2. The Extra Coil

As mentioned above, the classical Tesla coil uses two stages of voltage increase. Some coilers get a third stage of voltage increase by adding a magnifier coil, also called an extra coil, to their classical Tesla coil. This is illustrated in Fig. 6.
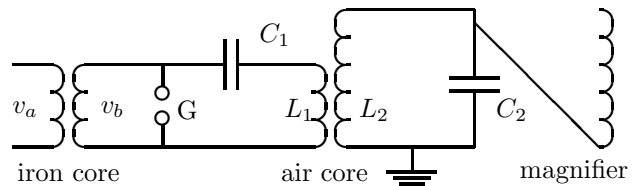


Figure 6: The Classical Tesla Coil With Extra Coil

The extra coil and the air core transformer are not magnetically coupled. The output (top) of the classical coil is electrically connected to the input (bottom) of the extra coil with a section of copper water pipe of large enough diameter that corona is not a major problem. A separation of 2 or 3 meters is typical.

Voltage increase on the extra coil is by transmission line action (field theory), or by RLC resonance (circuit theory), rather than the transformer action of the iron core transformer. Voltage increase on the air core transformer is partly by transformer action and partly by transmission line action. When optimized for extra coil operation, the air core transformer looks more like a transformer (greater coupling, shorter secondary)

than when optimized for classical Tesla coil operation.

Although not shown in Fig. 6 the extra coil depends on ground for the return path of current flow. The capacitance from each turn of the extra coil and from the top terminal to ground is necessary for operation. Impedance matching from the Tesla coil secondary to the extra coil is necessary for proper operation. If the extra coil were fabricated with the same size coil form and wire size as the secondary, the secondary and extra coil tend to operate as a long secondary, probably with inferior performance to that of the secondary alone. There are guidelines for making the coil diameters and wire sizes different for the two coils, but optimization seems to require a significant amount of trial and error.

In my quest for a better description of Tesla coil operation, I decided that the extra coil was the appropriate place to start. It looks like a vertical antenna above a ground plane, so there is some prior art to draw from. While the classical Tesla coil makes an excellent driver to produce long sparks, it is not very good for instrumentation and measurement purposes. There are just too many variables. The spark gap may be the best high voltage switch available today, but inability to start and stop on command, plus heating effects, make it difficult to use when collecting data.

I therefore decided to build a solid state driver. Vacuum tube drivers have been used for many years and several researchers have developed drivers using power MOSFETs, so this was not entirely new territory. I used this driver to measure the input impedance of several coils under various operating conditions, and compared these results with what theory I could find. This paper describes my results. Some data on my driver can be found on my web site, www.eece.ksu.edu/~gjohnson.

## 3. The Lumped RLC Model

There are two ways of modeling the Extra Coil: distributed (fields) and lumped (circuits). I spent considerable time with the distributed model, but was unable to predict all the interesting features. The lumped model is not perfect either, but may be easier to visualize. The system we are attempting to describe is shown in the next figure.

The voltage input $v_i$ at the base of the Tesla coil may be either a sine wave or a square wave. The square wave is composed of an infinite series of cosinusoids, the fundamental and all odd harmonics. The harmonics of the exciting wave will drive higher order resonances of the Tesla coil, if these resonances are harmonically related. It appears, at least for the coils I have built, that any
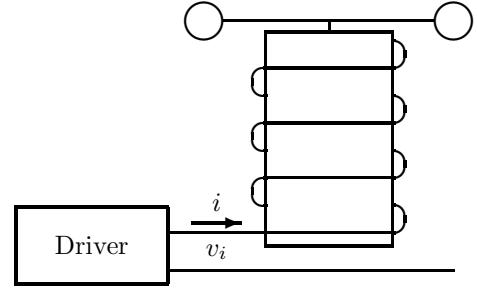


Figure 7: Drive for Tesla Coil

higher order resonances are not exact multiples of the fundamental frequency. That is, I apply a square wave of voltage to the feed point, and observe a current that looks sinusoidal at the fundamental frequency. The lumped RLC model automatically excludes higher order resonances, so if they are of significance, we must use a distributed model to describe them. I believe that higher order resonances are not a problem, at least not enough of a problem to exclude the use of the lumped model. The input impedance of the Tesla coil is the (fundamental) input voltage divided by the current $i$.

The lumped model used here is the series resonant RLC circuit shown in Fig. 8.
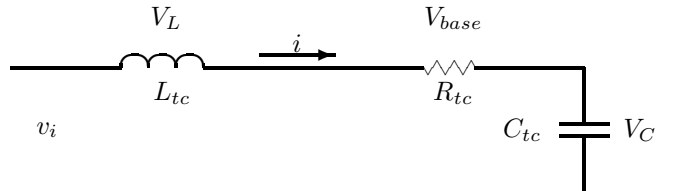


Figure 8: Tesla Coil with Series Resonant LC Circuit

The resonant frequency is given by

$$\omega_o = \frac{1}{\sqrt{L_{tc}C_{tc}}} \tag{1}$$

At resonance, the inductive reactance $\omega_o L_w$ is canceled by the capacitive reactance $-1/\omega_o C_{tc}$ so the current is

$$i = \frac{v_i}{R_{tc}} \tag{2}$$

The magnitude of the voltage across either the inductance or the capacitance is

$$V_C = iX_C = \frac{v_i}{R_{tc}}\frac{1}{\omega_o C_{tc}} = \frac{v_i}{\omega_o C_{tc} R_{tc}} \tag{3}$$

4

Books on circuit theory define the quality factor $Q$ as

$$Q = \frac{\omega_o L_{tc}}{R_{tc}} = \frac{1}{\omega_o C_{tc} R_{tc}} = \frac{1}{R_{tc}}\sqrt{\frac{L_{tc}}{C_{tc}}} \qquad (4)$$

so we can write

$$V_C = Q v_i \qquad (5)$$

We see that to get a large voltage on the toroid of a Tesla coil that it needs to be high $Q$. We need $R_{tc}$ small, $L_{tc}$ large, and $C_{tc}$ small. Let us look at ways of calculating or estimating these quantities.

## 4. Inductance

An empirical expression for the low-frequency inductance of a single-layer solenoid is [14, p. 55].

$$L_{tc} = \frac{r^2 N^2}{9r + 10\ell} \ \ \mu\text{H} \qquad (6)$$

where $r$ is the radius of the coil and $\ell$ is its length in inches. This formula is accurate to within one percent for $\ell > 0.8r$, that is, if the coil is not too short. It is known in the Tesla coil community as the Wheeler formula. The structure of a single-layer solenoid is almost universally used for the extra coil, so this formula is very important. In normal conditions (no other coils and no significant amounts of ferromagnetic materials nearby) it is quite adequate for calculating resonant frequency.

The classical Tesla coil has a short primary that is magnetically coupled into a taller secondary. The paper by Fawzi [5] contains the analytic expressions for the self and mutual inductances necessary for this case. A relatively simple numerical integration is required to get the final values. We can get the same results as the Wheeler formula by this numerical integration, but with somewhat less insight as to how inductance varies with the number of turns, and the length and radius of the coil.

## 5. Capacitance

$C_{tc}$ is much more difficult to calculate or to estimate with any accuracy. The capacitance value used to determine the resonant frequency of the Tesla coil is a combination of the capacitance of the coil and the capacitance of the top load, usually a sphere or a toroid, with respect to ground. As a practical matter, ground will be different in every Tesla coil installation. Easiest to model would be an outdoor installation (no walls or ceiling) with the coil setting on a large copper sheet. However, most coils are operated indoors without any copper sheet. Ground then consists of some combination of a concrete floor, electrical wiring, grounded light fixtures, and soil moisture. That is, the geometry necessary even for a numerical solution of capacitance is difficult to describe precisely.

To obtain the capacitance of a sphere to ground, we start with the capacitance of a spherical capacitor, two concentric spheres with radii $a$ and $b$ ($b > a$) as shown in Fig. 9.



Figure 9: Spherical Capacitor

It is not practical to actually build capacitors this way, but the symmetry allows an exact formula for capacitance to be calculated easily. This is done in most introductory courses of electromagnetic theory. The capacitance is given by [12, Page 165]

$$C = \frac{4\pi\epsilon}{1/a - 1/b} \qquad (7)$$

If the outer sphere is made larger, the capacitance decreases, but does not go to zero. In the limit as $b \to \infty$, the *isolated* or *isotropic* capacitance of a sphere of radius $a$ becomes

$$C_\infty = 4\pi\epsilon a \qquad (8)$$

Assuming a mean radius of 6371 km, the isotropic capacitance of the planet earth is 709 $\mu$F. A sphere of radius 0.1 m (a nice size for a small Tesla coil) would have an isotropic capacitance of 11.1 pF.

The other type of top load used for Tesla coils is the toroid. The dimensions of a toroid are shown in Fig. 10.
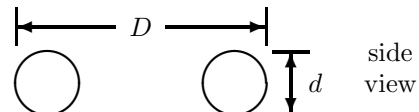


Figure 10: Toroid Dimensions

The analytic expression for the isotropic capacitance of a toroid involves Legendre functions of the first and

second order. It is *much* more difficult than the capacitance of a sphere. I discuss this expression at my web site, and give two corrections to formulas found in the Moon and Spencer textbook. For our purposes, empirical formulas for the capacitance of a toroid are more than adequate. The following are given by [13]

$$C_S = \frac{1.8(D-d)}{\ln(8(D-d)/d)} \qquad (d/D < 0.25) \qquad (9)$$

$$C_S = 0.37D + 0.23d \qquad (d/D > 0.25) \qquad (10)$$

where $D$ is the toroid major diameter, outside to outside, in cm, $d$ is the toroid minor diameter in cm, and the capacitance is given in pF.

Empirical equations for the isotropic capacitance of a coil were developed many years ago by Medhurst. These can be expressed in several different versions, to meet different needs. The simplest expression for the isotropic capacitance of a cylindrical coil of wire, with diameter $D$ and coil length $\ell$, is

$$C_M = HD \ \text{pF} \qquad (11)$$

where $D$ is in cm, and $H$ is a multiplying factor that equals 0.51 for $\ell/D = 2$, 0.81 for $\ell/D = 5$, and varies linearly between 0.51 and 0.81 for $\ell/D$ between 2 and 5. Most coilers prefer values for $\ell/D$ between 3.5 and 4.5, so this linear range is adequate for most purposes.

An expression for $H$ that works for $\ell/D$ between 2 and 8 is

$$H = 0.100976\frac{\ell}{D} + 0.30963 \qquad (12)$$

Another expression for $H$ that works for $\ell/D$ between 1 and 8 is

$$\begin{aligned} H &= 0.0005(\frac{\ell}{D})^4 - 0.0097(\frac{\ell}{D})^3 + 0.0648(\frac{\ell}{D})^2 \\ &\quad -0.0757(\frac{\ell}{D}) + 0.4723 \end{aligned} \qquad (13)$$

We now have expressions for the isotropic capacitance $C_S$ of a toroid (or sphere) and the isotropic capacitance $C_M$ of a coil. We want to somehow use these expressions to find the effective capacitance $C_{tc}$ for the Tesla coil with the toroid (or sphere) on top the coil. Unfortunately, life is not that simple. As we bring the

coil near a ground plane, the capacitance increases. As we add walls and a ceiling, the capacitance increases some more. The same is true for the toroid. The capacitance increases as it is brought to the vicinity of a ground plane.

But if we want the isotropic capacitance of the combination of the coil and the toroid (the two items assembled at a remote location), shielding occurs such that the effective capacitance is less than the sum of the two isotropic capacitances. We have two opposing trends. The actual isotropic Tesla coil capacitance is smaller than the sum $C_M + C_S$ but when the coil and toroid are brought near grounded surfaces, the effective capacitance to be used in calculating resonant frequency will increase. The opposing trends suggests that $C_{tc}$ might be within 20% of $C_M + C_S$ for most Tesla coils. The resonant frequency is related to the square root of $C_{tc}$ so a 20% error in capacitance results in only a 10% error in resonant frequency.

The main benefit of the expressions for $C_M$ and $C_S$ is that they allow us to do 'what if' analyses relatively quickly. Questions about the effect of changing coil diameter, coil length, or toroid diameter can be answered with adequate accuracy.

It is possible to calculate $C_{tc}$ numerically using Gauss's Law. If one is careful about measuring and entering all the dimensions and the locations of grounded surfaces, one should get a value for $C_{tc}$ well within 5% of the correct value. There are programs available in the Tesla coil community that do this.

## 6. Copper Resistance

$R_{tc}$ includes all the different types of losses observed in an actual Tesla coil, including radiation losses (the coil putting some of the input power into Hertzian waves being radiated into space) and dielectric losses (heat produced in the coil form and the wire insulation). The largest component of $R_{tc}$ in a well-built coil is the 'copper' resistance $R_{cu}$. (Most Tesla coils are wound with copper wire, but other conductors could be used as well. The 'copper' resistance is the effective resistance of the conducting metal, excluding other types of losses.) This is found in three steps: First we find the dc resistance $R_{dc}$ given the length and diameter of the wire, and the temperature. We can either look up the resistance per unit length in a table and multiply by the length, or we can simply use a ohmmeter.

Second, we find the ac resistance of the same wire in one single straight length (not in a coil). $R_{ac}$ is greater than $R_{dc}$ because of the skin effect that causes less of the total current to flow in the center of the wire. We

6

can write

$$R_{ac} = K_{skin}R_{dc} \tag{14}$$

where the multiplying factor due to skin effect is greater than unity and less than perhaps three. The general procedure for finding this multiplying factor is found in many electromagnetic theory books.

Third, we find the ac resistance of the wire when formed into a coil. The resistance is increased because of the proximity effect. I have not found a treatment of the proximity effect for a solenoid in a textbook. I found two papers that deal with this effect, by Medhurst [10] (of Medhurst capacitance fame), and Fraga [6]. Neither paper deals with the typical values of skin depth $\delta$ versus wire diameter found in Tesla coils. Medhurst looked at the high frequency case where $b \gg \delta$ while Fraga looked at the low frequency case ($b \leq \delta$). Tesla coils are usually operated at frequencies where the wire radius will be between one and five skin depths.

We might define a Medhurst copper resistance $R_{cu,M}$ and a Fraga copper resistance $R_{cu,F}$ from these two papers where

$$R_{cu,M} = K_M R_{ac} \tag{15}$$

$$R_{cu,F} = K_F R_{ac} \tag{16}$$

where $K_M$ and $K_F$ are looked up in Table 1.

Table 1: Experimental values of $K_M$ and $K_F$ (last column), the ratio of high-frequency coil resistance to the resistance at the same frequency of the same length of straight wire.

| $d/z_1$ | $\ell_w/D$ | | | | | | $K_F$ |
|---|---|---|---|---|---|---|---|
| | 1 | 2 | 4 | 6 | 8 | $\infty$ | |
| 1 | 5.55 | 4.10 | 3.54 | 3.31 | 3.20 | 3.41 | 3.19 |
| 0.9 | 4.10 | 3.36 | 3.05 | 2.92 | 2.90 | 3.11 | 3.03 |
| 0.8 | 3.17 | 2.74 | 2.60 | 2.60 | 2.62 | 2.81 | 2.86 |
| 0.7 | 2.47 | 2.32 | 2.27 | 2.29 | 2.34 | 2.51 | 2.67 |
| 0.6 | 1.94 | 1.98 | 2.01 | 2.03 | 2.08 | 2.22 | 2.48 |
| 0.5 | 1.67 | 1.74 | 1.78 | 1.80 | 1.81 | 1.93 | 2.26 |
| 0.4 | 1.45 | 1.50 | 1.54 | 1.56 | 1.57 | 1.65 | 2.03 |
| 0.3 | 1.24 | 1.28 | 1.32 | 1.34 | 1.34 | 1.40 | 1.75 |

In this table, $\ell_w$ is the coil winding length, $D$ is the coil diameter, $d$ is the diameter of the copper wire,

and $z_1$ is the center-to-center spacing between adjacent turns, all in consistent units. This table indicates that the proximity effect can easily double or triple the measured input resistance over that predicted by $R_{ac}$ for a straight wire of the same length.

We now need to return to a discussion of the skin effect. An expression for skin depth can be derived as

$$\delta = \frac{1}{\sqrt{\pi f \mu \sigma}} \tag{17}$$

where $f$ is the frequency in Hz, $\mu$ is the permeability of the conductor ($4\pi \times 10^{-7}$ for nonferromagnetic materials), and $\sigma$ is the conductivity.

The skin depth for copper at 20$^o$C is

$$\delta = \frac{0.066}{\sqrt{f}} \quad \text{m} \tag{18}$$

Most introductory electromagnetic theory books derive the expression for ac resistance as

$$R_{ac} = R_{dc}\frac{b}{2\delta} \tag{19}$$

where $b$ is the radius of the wire and $\delta$ is the skin depth, in consistent units. This equation is only valid for $\delta \ll b$. As might be expected, this excludes most Tesla coils, so we must find other expressions.

A typical analytic approach is to start with Maxwell's Equations and write a differential equation for the current density inside the wire. The solution of this differential equation is a Bessel function. Things start to get tedious as one tries to keep track of the real and imaginary parts of the Bessel function (the ber and bei functions). I show some of the details at my web site.

The approximations developed by Terman [14], who has a detailed discussion of this topic, will be quite sufficient for our purposes. He defines $R_{ac}$ in terms of a parameter $x$, where

$$x = \pi d\sqrt{\frac{2f}{\rho(10^7)}} \tag{20}$$

for nonmagnetic materials. Here, $d$ is the conductor diameter in meters, $f$ is the frequency in Hz, and $\rho$ is the resistivity in ohm meters. As $x$ gets very small, due to either low frequency or small wire, the ac resistance approaches the dc resistance. Above about $x = 3$, $R_{ac}/R_{dc}$ varies essentially linearly with $x$ according to the expression

$$\frac{R_{ac}}{R_{dc}} = 0.3535x + 0.264 \qquad (x > 3) \quad (21)$$

Terman gives the following tabular values of $R_{ac}/R_{dc}$ for $x$ between 0 and 3.

Table 2: $R_{ac}/R_{dc}$ for various values of $x$.

| $x$ | $R_{ac}/R_{dc}$ | $x$ | $R_{ac}/R_{dc}$ |
|-----|------|-----|------|
| 0   | 1.0000 | 1.5 | 1.026 |
| 0.5 | 1.0003 | 1.6 | 1.033 |
| 0.6 | 1.0007 | 1.7 | 1.042 |
| 0.7 | 1.0012 | 1.8 | 1.052 |
| 0.8 | 1.0021 | 1.9 | 1.064 |
| 0.9 | 1.0034 | 2.0 | 1.078 |
| 1.0 | 1.005  | 2.2 | 1.111 |
| 1.1 | 1.008  | 2.4 | 1.152 |
| 1.2 | 1.011  | 2.6 | 1.201 |
| 1.3 | 1.015  | 2.8 | 1.256 |
| 1.5 | 1.020  | 3.0 | 1.318 |

For copper, $\rho = 1.724 \times 10^{-8}$ ohm meters. For those of us still using wire tables in English units, where wire diameters are given in mils (1 mil = 0.001 inch), Terman [14] has reduced the expression for $x$ to

$$x = 0.271 d_m \sqrt{f_{MHz}} \qquad (22)$$

where $d_m$ is the wire diameter in mils and $f_{MHz}$ is the frequency in MHz.

For example, I used 482 meters of 14 ga copper wire to wind a coil. The dc resistance is 3.99 $\Omega$ at 20$^o$C. The nominal diameter of 14 ga wire is 64.08 mils. Assume the resonant frequency to be 160 kHz. We calculate $x$ as

$$x = 0.271(64.08)\sqrt{0.16} = 6.946$$

The ac resistance of the wire in the coil (assuming the wire is uncoiled and is supported in one straight line) is then

$$R_{ac} = 3.99(0.3535(6.964) + 0.264) = 10.85 \quad \Omega$$

We see that skin effect makes a significant difference in resistance, especially where larger wire sizes or higher frequencies are used.

The diameter $D$ of this coil was 0.396 m, the winding length $\ell_w$ was 1.166 m, the wire diameter $d$ was 64.08 mils or 1.628 mm, and the number of turns was 387. The center-to-center spacing between adjacent turns $z_1$ was $z_1 = \ell_w/(N-1) = 3.02$ mm. The quantity $d/z_1 = 1.628/3.02 = 0.54$. The quantity $\ell_w/D = 1.166/0.396 = 2.94$. By interpolation in Table 1, $K_M$ is found to be 1.85. Therefore, the predicted ohmic resistance $R_{cu,M}$ of the coil would be $(1.85)(10.85) = 20$ $\Omega$ (at sufficiently high frequencies). Interpolation in the last column of Table 1 gives $K_F = 2.348$ and $R_{cu,F} = (2.348)(10.85) = 25.5\Omega$. The measured input resistance is about 23 $\Omega$ at resonance. This measured resistance includes dielectric losses, radiation losses, etc. in addition to ohmic losses. The Medhurst estimate $R_{cu,M}$ allows 3 $\Omega$ for these losses, which is probably not far from reality. The Fraga estimate $R_{cu,F}$ is at least 10% too high, and perhaps 20% too high for this particular coil.

The Medhurst estimate appears to be better for some coils, while the Fraga estimate seems better for other coils. I tested nine different coils, eight with three different top loads to get three different frequencies, so I had a total of 25 cases where I could compare the calculated $R_{cu,M}$ and $R_{cu,F}$ with the measured $R_{tc}$. $R_{cu,M}$ was less than $R_{tc}$ by a 'reasonable' amount 15 times, while $R_{cu,F}$ was less than $R_{tc}$ by a 'reasonable' amount 11 times. When both calculated values were greater than the measured, $R_{cu,F}$ was closer to the measured case twice, while $R_{cu,M}$ was closer three times. There were six cases (all three frequencies for two short, fat coils) where $R_F$ was less than $R_{tc}$ by an 'unreasonable' amount. One example was a coil wound with 16 gauge wire on a barrel where I measured $R_{tc} = 93.1\Omega$, and calculated $R_{cu,M} = 80.9\Omega$ and $R_{cu,F} = 51.1\Omega$. The conclusion seems to be that as long as we stay away from short, fat coils, either Medhurst or Fraga estimates will be in the right ball park.

Table 3 illustrates a common but non-intuitive observation in the Tesla coil community, that coils with a smaller wire size (higher resistance per unit length) may work as well as coils wound with larger wire. We see this as we compare coils 18T and 22T. Coil 18T is tight wound with 18 gauge Essex copper magnet wire, coated with what they call Heavy Soderon. Coil 22T is tight wound with 22 gauge tinned copper hook-up wire, with what I assume to be PVC insulation. The thicker insulation means the copper of each turn has a greater spacing, which reduces the proximity effect. The Medhurst factor $K_M$ drops from 3.15 to 1.62 between the two coils, due mostly to this greater spacing.

The dc resistance of coil 22T is twice that of coil 18T, so the natural assumption would be that $R_{tc}$ would be larger for coil 22T. However, the thinner wire is more

Table 3: Predicted and Measured Coil Resistance for Several Coils

| | 14S | 18T | 22T |
|---|---|---|---|
| $d$, mm | 1.628 | 1.024 | .6439 |
| $D$, meters | .396 | .214 | .214 |
| $\ell_w$, meters | 1.166 | .881 | .945 |
| wire, meters | 482 | 534 | 424 |
| turns $N$ | 387 | 794 | 631 |
| $L_{tc}$, mH | 17.2 | 29.1 | 17.2 |
| $C_M$, pF | 23.95 | 15.45 | 16.08 |
| $K_M$ | 1.85 | 3.15 | 1.62 |
| $R_{dc}$ | 3.99 | 11.2 | 22.4 |
| $f_0$, kHz | 247.6 | 236.9 | 301.5 |
| $R_{cu,F}$ | 29.99 | 67.55 | 65.94 |
| $R_{cu,M}$ | 24.7 | 76.50 | 58.38 |
| $R_{tc}$ | 24.5 | 70.5 | 47.0 |
| $f$ | 217.3 | 176.1 | 227.9 |
| $R_{cu,F}$ | 28.10 | 58.23 | 56.76 |
| $R_{cu,M}$ | 23.13 | 66.52 | 51.57 |
| $R_{tc}$ | 25.6 | 65.9 | 46.7 |
| $f$ | 158.8 | 122.5 | 158.1 |
| $R_{cu,F}$ | 24.02 | 48.57 | 45.76 |
| $R_{cu,M}$ | 20.06 | 57.03 | 44.56 |
| $R_{tc}$ | 24.5 | 58.1 | 42.4 |

effective in its use of available cross section. $R_{ac} = 24\Omega$ for coil 18T at 236.9 kHz, and 35.8 $\Omega$ for coil 22T at 301.5 kHz, a difference of 49% rather than 100%. Then when we multiply by $K_M$, we get $R_{cu,M} = 76.50\Omega$ for coil 18T, and 58.38 $\Omega$ for coil 22T. Coil 22T has 200% of the dc resistance of coil 18T, but only 76% of the effective resistance during operation at frequency $f_0$. The proximity effect increases the resistance of both coils above the ac resistance value, but far more for the tighter effective spacing of coil 18T, so coil 22T is actually the superior coil for Tesla coil activity. The same observation holds as larger top loads are used, driving the resonant frequency down.

The measured values for $R_{tc}$ are even less than the Medhurst predicted values, 11 $\Omega$ less for coil 22T and 6 $\Omega$ less for 18T at frequency $f_0$. It is always possible that my experimental technique was lacking on these two tests. I prefer to think, however, that the assumptions made by Medhurst do not match reality for these two coils, so that the 'correct' proximity factors would be a little less than shown in Table 1 for these particular coil parameters.

## 7. Other Losses

We are now ready to discuss (at least qualitatively) other losses besides those due to copper resistance. These are illustrated in the next figure.
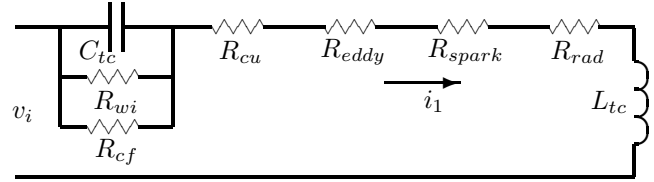


Figure 11: Detailed Lumped Model of Tesla Coil

$R_{rad}$ refers to the power radiated away into space as an electromagnetic wave. In all my tests, $R_{rad}$ was very close to zero, probably not larger than 0.01 $\Omega$. I was unable to detect a signal from the coil more than perhaps 100 m away, using a high quality short wave receiver that functioned down to 150 kHz. A Tesla coil is a *really* bad antenna.

$R_{eddy}$ refers to eddy current losses in the toroid (or sphere) on top the coil, and in any other conducting surfaces nearby. Eddy current losses can be substantial in some engineering applications. A power frequency transformer built of solid steel rather than thin steel laminations would melt quickly! A spun aluminum toroid exposed to the magnetic field of the Tesla coil current will certainly have eddy currents. There has been more than one serious Tesla coiler who has been tempted to cut radial slots into the toroid to reduce these eddy currents.

I built a toroid of 0.25 inch copper tubing pieces on insulating disks, connected together at one point by a conducting disk. The ends were placed into heat shrink tubing, which was then shrunk to hold the ends a fixed small distance apart. This toroid was then compared with a spun aluminum toroid of similar capacitance, and also with a smaller toroid made of one inch copper tubing with diameter slightly greater than that of the coil form. The smaller toroid was an attempt to get a shorted turn as near to the coil as possible. It lacked the capacitance to be an effective toroid for long sparks, of course. I could not find any significant difference in input impedance between the insulated toroid and the spun aluminum toroid. The shorted copper ring, however, had about 10% higher input impedance than the toroid that was not a shorted turn. This suggests that you would not notice any improvement if you cut your beautiful spun aluminum toroid into pieces to eliminate eddy currents. The effect is there, and can be measured if one really works at it, but is not that significant in most situations.

Overall, my tests indicated that $R_{eddy}$ is no more than a few percent of $R_{TC}$. If a little thought is given to separation of conducting materials from the immediate vicinity of the coil, eddy current losses can be ignored.

The model indicates that when a spark occurs, the equivalent resistance $R_{spark}$ increases from zero to some finite value, so the input resistance *increases* during a spark. This is exactly what happens experimentally. The input current *drops* when the spark starts, for a constant supply voltage.

The copper, eddy current, and radiation losses are all proportional to the square of the *current* in the coil. The losses in the hot plasma of the spark are such that the spark losses may not be proportional precisely to the *square* of the current, but are definitely related to some function of the current. On the other hand, the dielectric losses are proportional to the square of the *voltage* across the coil. I try to show that with resistors across the capacitance $C_M$. There are two distinct dielectrics, the coil form and the wire insulation, represented by $R_{cf}$ and $R_{wi}$. Air forms a third dielectric, but dry air is basically lossless. Humidity in the air does add losses, but this humidity soaks into the coil form and wire insulation, increasing the losses there. I did not try to distinguish between losses in humid air and losses of the coil and coil form.

For single-frequency, steady-state operation, the parallel combination of a capacitor and two resistors can be modeled as a series capacitor and resistor, call it $R_{die}$. This is straightforward Circuit Theory I, but a bit tedious. We write an expression for the parallel impedance of $R_{cf}$, $R_{wi}$, and the capacitance, rationalize it, and simplify the real term. We assume that the parallel resistances are much larger than the capacitive reactance, as they will be for any coil with acceptable losses. Calculation details can be found at my web site.

One line of analysis shows that $R_{die}$ varies as $1/f^2$. Generally speaking, $R_{ac}$ increases as $\sqrt{f}$, and $R_{eddy}$ increases as $f^2$. $R_{rad}$ will increase at a rate somewhere between $f$ and $f^2$. $R_{spark}$ can be ignored below the spark inception voltage. Depending on which terms are dominant loss terms, we may not see a pronounced change in input impedance with frequency. That has been my experience. Input impedance will drift from day to day, (mostly with humidity), but there is no obvious frequency dependence. Of course, other things are happening. We know that $R_{ac}$ increases with temperature, while $R_{die}$ increases with humidity. If these were the only factors, we would expect a cold, dry winter day to have the lowest impedance, and a hot, muggy day to have the highest impedance and the worst performance. In cases where moisture is a factor, performance might improve after a period of operation which caused the coil form to heat up and dry out.

Effects of humidity are shown in two sets of input impedance data in Table 4 for 3/17/01 and 4/6/01. The coils were located in the bay of a large Morton building (a metal skin building, not heated or air conditioned, that might be used for storage of tractors and other agricultural equipment). The Tesla coil driver and other test equipment were located in a climate-controlled room built into a corner of the Morton building. The 3/17/01 data were collected when the bay temperature was about $9^oC$ and the relative humidity was about 28%. On 4/6/01 the temperature was about $17^oC$ and the relative humidity was 100%. It had been damp all week with heavy fog the day before. It would be rare for a Tesla coil to be operated with significantly lower relative humidity or total moisture in or on the dielectrics than the conditions of 3/17/01, and likewise for more moisture than 4/6/01.

Table 4: $R_{tc}$ Measured on Two Different Days

| Coil | $f$ | $R_{tc}$ 3/17/01 | $R_{tc}$ 4/6/01 |
|------|------|------|------|
| 14S | 249.1 | 24.5 | 27.6 |
| 14T | 266.1 | 43.5 | 45.5 |
| 16B | 145.5 | 93.1 | 175.8 |
| 18T | 242.6 | 70.5 | 75.7 |
| 20T | 183.6 | 94.2 | 100.0 |
| 22T | 307.0 | 47.0 | 53.4 |
| 22B | 148.3 | 73.0 | 126.7 |

We see that two of the coils experienced large changes in $R_{tc}$, coils 16B and 22B. Both coils used a plastic barrel as a coil form that I thought was polyethylene. I got the barrels at the local recycling plant. Coil 22B used the same type of wire as coil 22T which was wound on a piece of PVC, so the difference in $R_{tc}$ between these two coils had to be the coil form. These results indicate that some coil forms are worse than others. These barrels evidently soak up water in amounts sufficient to raise the input impedance by a factor of two.

Coils 14T, 18T, 20T, and 22T were wound on PVC while coils 14S and 18B were wound on polyethylene. Only coil 20T had any type of coating put on top the winding (polyurethane). Both PVC and polyethylene appear to have about the same increase in $R_{tc}$ with humidity, so it is hard to argue that one should spend more money on the more expensive polyethylene.
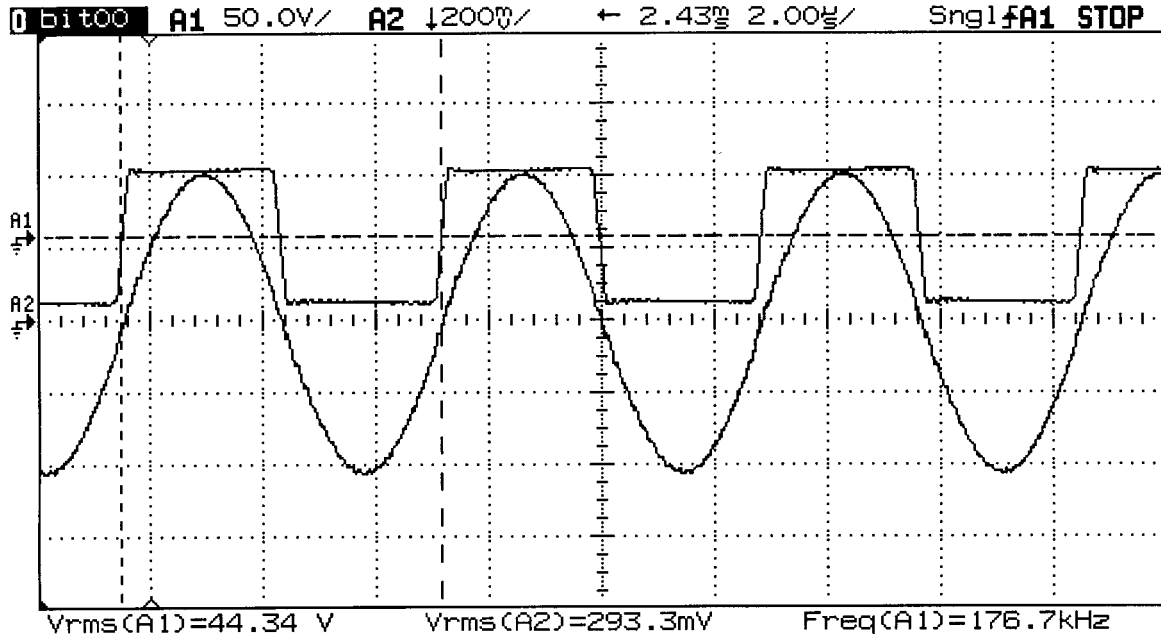
Figure 12: Square wave of voltage, sine wave of current at base of coil 12T below breakout.

As long as one stays with good quality coil forms, it appears that high humidity will raise $R_{tc}$ by 5–10% from the low humidity case. This variation of $R_{tc}$ with humidity makes it pointless to do more analytical or computational work to get better estimates of $R_{cu,M}$ or $R_{cu,F}$, since we appear to be within the 5–10% range of accuracy for most cases already.

In my opinion, a complete distributed model will not be any better in dealing with skin effect, proximity effect, and dielectric losses, and would certainly be more of a programming problem. The one thing that this lumped model cannot deal with directly is the displacement current effect. In a lumped model, the current must be the same at all points of the circuit. Actually the current varies from one point in the coil to another point, due to capacitive and inductive effects. It is counter-intuitive, but the current may actually increase from the base feed point to about a third of the way up the coil before starting a monotonic decrease to a minimum at the top of the coil. A distributed model can determine the actual current distribution, which can then be used to find a predicted effective resistance of the coil. The computational effort is much greater than the table look-up techniques used to get $R_{cu,M}$ and $R_{cu,F}$ for the lumped case. Whether the accuracy of the predicted resistance is sufficiently improved to justify the extra effort is open to question.

## 8. Impedance During Sparking

I calculated the input impedance of the Tesla coil from measured values of $v_i$ and $i_1$, at or very near resonance. I would apply a square wave voltage from my driver and measure it and the resulting current with a HP54645D oscilloscope. If the voltage was below that necessary for a spark to occur, current would rise to a steady-state value. Steady-state waveforms are illustrated in Figure 12.

Voltage is actually the voltage output of a 10:1 voltage divider. The vertical scale for channel A1 is thus 500 V/div rather than 50. At the lower left of the screen image we see Vrms(A1)=44.34 V. The rms value would actually be 443.4 V. The rms of a perfect square wave is the same as the peak value, so I am applying a voltage of approximately ±443.4 V to the coil.

The current waveform is the voltage across a 20 mΩ resistor. The current corresponding to a voltage of 293.3 mV is

$$i_1 = \frac{V}{R} = \frac{293.3\text{mV}}{20\text{m}\Omega} = 14.67 \quad \text{A} \qquad (23)$$

The combination of a square wave voltage and a sinusoidal current is different from what we are used to, so we need to go back to circuit theory to make sure we have all the correct multiplying factors.

11

Suppose that we apply a sinusoidal voltage $V_p \sin \omega t$ to a non-inductive resistor. The resulting current is $I_p \sin \omega t$. The average power is

$$P_{ave} = \frac{1}{\pi} \int_0^\pi V_p I_p \sin^2 \theta d\theta = \frac{V_p}{\sqrt{2}} \frac{I_p}{\sqrt{2}} = \frac{V_p I_p}{2} = V_{ac} I_{ac} \tag{24}$$

When the square wave voltage produces a sinusoidal current, the integral for average power becomes

$$\begin{aligned} P_{ave} &= \frac{1}{\pi} \int_0^\pi V_p I_p \sin \theta d\theta = \frac{2}{\pi} V_p I_p \\ &= \frac{2}{\pi} V_p (\sqrt{2} I_{ac}) = 0.9 V_{ac} I_{ac} \end{aligned} \tag{25}$$

For this case, the average power is no longer the simple product of rms voltage and rms current (as for dc and single frequency sinusoids), but has a 0.9 multiplying factor. The difference is due to the fact that the square wave voltage is composed of an infinite series of harmonics (fundamental, third, fifth, etc.). Each harmonic contributes to the rms value of the square wave. The current has no harmonics, so the higher voltage harmonics do not produce any contribution to the apparent power.

Actually the product $0.9 V_{ac} I_{ac}$ is the apparent power $S$ for these two waveforms, which happens to be equal to the average power when the waves are in phase. If there is a phase shift, $P_{ave}$ will be less than $S$ by a factor $\cos \theta$, where $\theta$ is the phase angle between the two waves. I can readily determine $S$ from the product of rms voltage and rms current (and a 0.9 multiplying constant). I always try to operate with voltage and current in phase, so $S$ can be used as an approximation for $P_{ave}$.

The average power being applied to the coil in Fig. 12 is approximately

$$P_{ave} = 0.9 V_{ac} I_{ac} = (0.9)(443.4)(14.67) = 5854 \quad \text{W} \tag{26}$$

Fig. 13 shows the voltage applied to another Tesla coil and the resulting current for about 4.5 ms. The voltage is A1 at the top of the figure and the current is A2 at the bottom. Operation is well below breakout. The driver is supplying voltage from storage capacitors for about 2.1 ms. Current builds up as predicted by either transmission line theory or lumped RLC analysis. Current builds nearly linearly at first, then the rate of

increase slows as losses increase. Current will hit its limit when the input power is equal to the losses, in this case between 2 and 3 ms after start.

As current increases, the voltage drop across the MOSFETs/IGBTs and the droop in the electrolytic capacitors becomes greater. The decrease in voltage applied to the Tesla coil is not great, but is most easily noticed when the gate drives are turned off at the 2.1 ms point. Energy stored in the Tesla coil has to be dissipated somehow. Instead of power flowing from inverter to coil, it now flows in the opposite direction. Voltage is constrained by the built-in diodes of the IGBTs. Power supply capacitors are now being charged instead of discharged. All the voltage drops in wiring and the IGBTs reverse in sign. We therefore see a small step increase in voltage when the gate drive signals are removed.

About 0.6 ms after gate drive turn-off, the stored energy is no longer able to force the IGBT diodes into forward conduction. Without a power supply affecting the circuit, we now have a classic RLC ring down. Both voltage and current are decreasing exponentially. During this portion of the cycle, the IGBTs are acting as capacitors.

When the supply voltage is increased, a spark occurs when the toroid reaches a sufficient voltage. Figure 14 shows the current building up slowly until spark initiation at about 1.4 ms and then a more rapid decline. The jagged appearance of the wave envelope is due to the scope's algorithm to select representative points from the long waveform data set and does not imply that the current is experiencing rapid excursions. When one spreads out the waveform, it can be seen that the current looks as well behaved as the current in Figure 12 except that it grows by a small amount each cycle until breakout.

One cycle at 176.7 kHz lasts for about 5.66 $\mu$s. If the spark starts at 1400 $\mu$s, then it took $1400/5.66 = 247$ cycles to get to breakout. Just before breakout, the voltage was about 604 V and the current was 17.1 A. I had to expand the waveforms near the 1400 $\mu$s point to get these values. The instantaneous power (the average power at that instant) was about 9.3 kW. The current during the spark was about 4 A.

I increased the voltage about 50% and got the current waveform in Figure 15. The spark now starts at about 0.93 ms. Just before breakout, the voltage was about 914 V, the current was 21.5 A, and the instantaneous power was about 17.7 kW. The current during the spark remained at about 4 A.
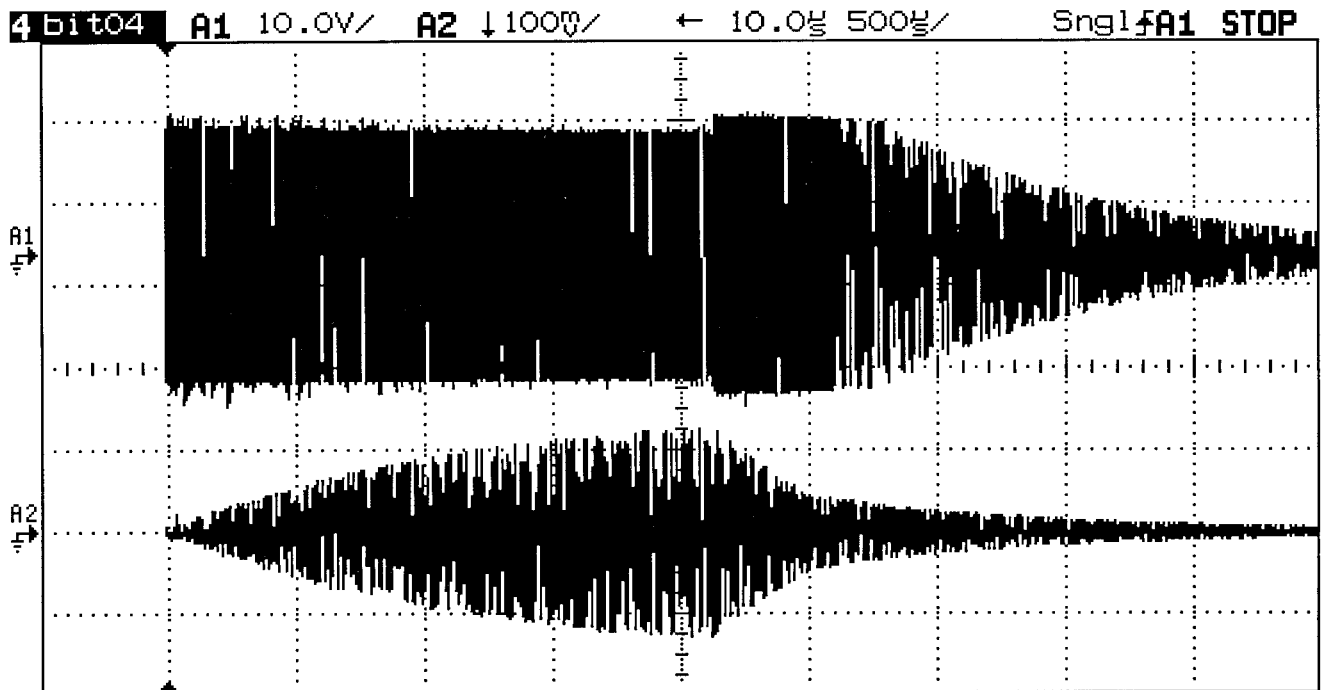
Figure 13: Tesla Coil Voltage and Current Waveforms

The coil appears to operate as a constant-current device in breakout. Both the input dc current and the ac current into the coil stay about constant, perhaps even decreasing a little, as the supply voltage is increased. The input impedance increases proportional to the input voltage, in order for the current to remain constant. This is somehow caused by the dynamics of the hot plasma in the discharge. I do not have a detailed explanation.

The 'inertia' of the electrons and ions on and around the toroid play an important part in the length of the streamer. Increasing the supply voltage causes the current and the energy stored in the coil to build up more rapidly. This more rapid growth allows less time for the breakdown of air to occur, with the result of more energy stored in the coil when breakdown does occur. This greater energy translates to a longer streamer.

The nature of the discharge process causes variability in the exact amount of current necessary to produce a streamer for any given shot. At lower levels of voltage, a streamer might be produced one time out of ten applied pulse trains. The time lag between start and discharge might vary by a factor of two, probably depending on the chance arrival of a gamma ray or a beta particle from a radioactive decay. At higher levels of voltage, one gets a streamer each pulse train, but the time from start to discharge, and the resultant power input just before discharge, can still easily vary by 10%.

If power continues to be supplied to the discharge after the onset, the discharge does not get longer, but instead gets 'fatter'. Figure 16 shows two streamers where the driving voltage was removed soon after the streamers started. The streamers have a thin, violet, anemic appearance. Figure 17 shows two different streamers where the driving voltage was left in place for perhaps 2 ms after the onset. The streamers now appear richer, fuller, and whiter. The trend continues with even longer applied voltage as shown in Fig. fig:fat.

The camera is able to show details that the eye cannot follow. The streamer does not get uniformly thicker, but rather shows charge leaving the main discharge path at all the 'corners' of the original discharge path and then curving back toward the main path. It is almost as though the charge carriers in the discharge have inertia, such that they want to continue traveling in a straight line when a 'corner' is encountered. If the only forces involved were the Coulombic forces, the es-

13
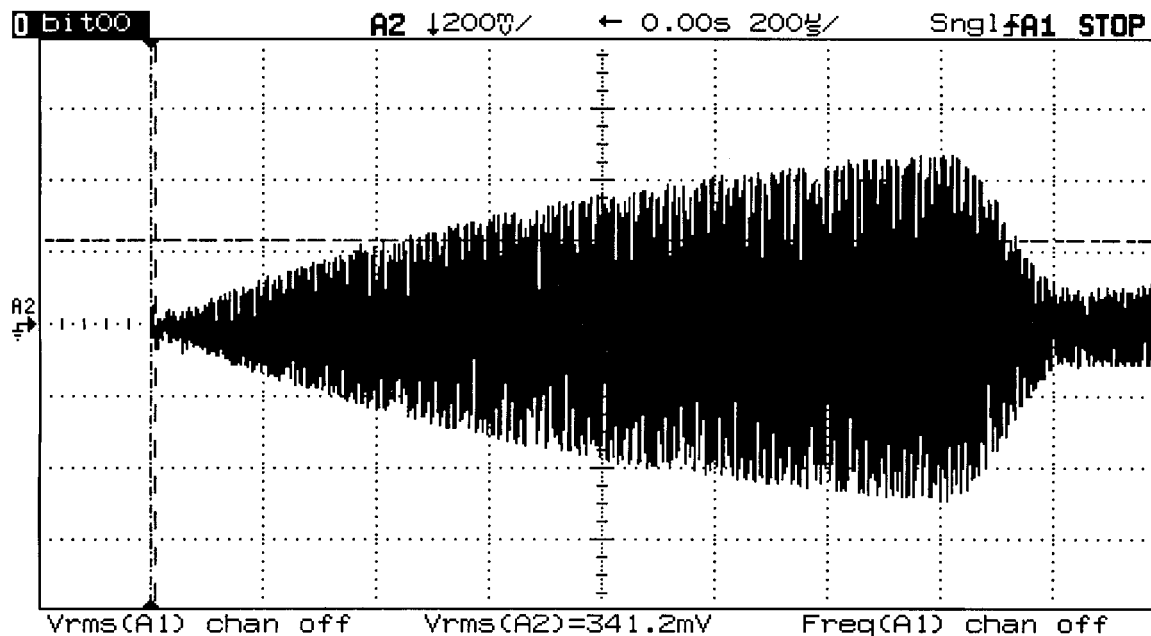
Figure 14: Current Waveform with Voltage = ±604 V

caping charges would not be drawn back to the main path. But there are also Amperian forces. Two parallel currents experience an attractive force. Evidently these Amperian forces are stronger than the Coulombic forces in this case. I have not made any attempt to quantify these forces.

A casual examination of these (and many other) photos suggests that the escaping charges travel in a spiral around the main path before returning to it. This might be an optical illusion. It would require two or more cameras orthogonal to the streamer and each other to prove or disprove this appearance. This would be something to check in any further research.

I put a bump on the toroid so all sparks started from the same point, and placed a sheet of plastic with concentric circles behind the bump. I then set the driver to produce a few sparks per second and observed the length of the discharges to air. I would also determine the average power input just before discharge. Then I would increase the voltage and repeat the process. I found the spark length to be related to the square root of power according to the formula

$$\ell_s = 0.17\sqrt{P} \qquad \text{inches} \qquad (27)$$

where $P$ is measured in watts. For the current waveforms of Figure 14 and Figure 15 the corresponding spark lengths were 16.4 and 22.6 inches. If the formula

remains valid at higher powers, an input power of 1 MW would produce a spark length of 14 feet. If we use IGBTs that can safely deliver 50 A at Tesla coil frequencies, this requires a supply voltage of ±20,000 V. If the individual IGBTs have a working voltage of 1000 V, then a chain of 20 IGBTs would be necessary for each side of the power supply. I will not predict that such a driver cannot or will not be built. I will just say that getting *long* sparks from a solid state driver is *not* easy!

# References

[1] Corum, J. F. and K. L. Corum, "A Technical Analysis of the Extra Coil as a Slow Wave Helical Resonator", *Proceedings of the 1986 International Tesla Symposium*, Colorado Springs, Colorado, July 1986, published by the International Tesla Society, pp. 2-1 to 2-24.

[2] Corum, James, F., Daniel J. Edwards, and Kenneth L. Corum, *TCTUTOR - A Personal Computer Analysis of Spark Gap Tesla Coils*, Published by Corum and Associates, Inc., 8551 State Route 534, Windsor, Ohio, 44099, 1988.

[3] Couture, J. H., *JHC Tesla Handbook*, JHC Engineering Co., 19823 New Salem Point, San Diego, CA, 92126, (1988).
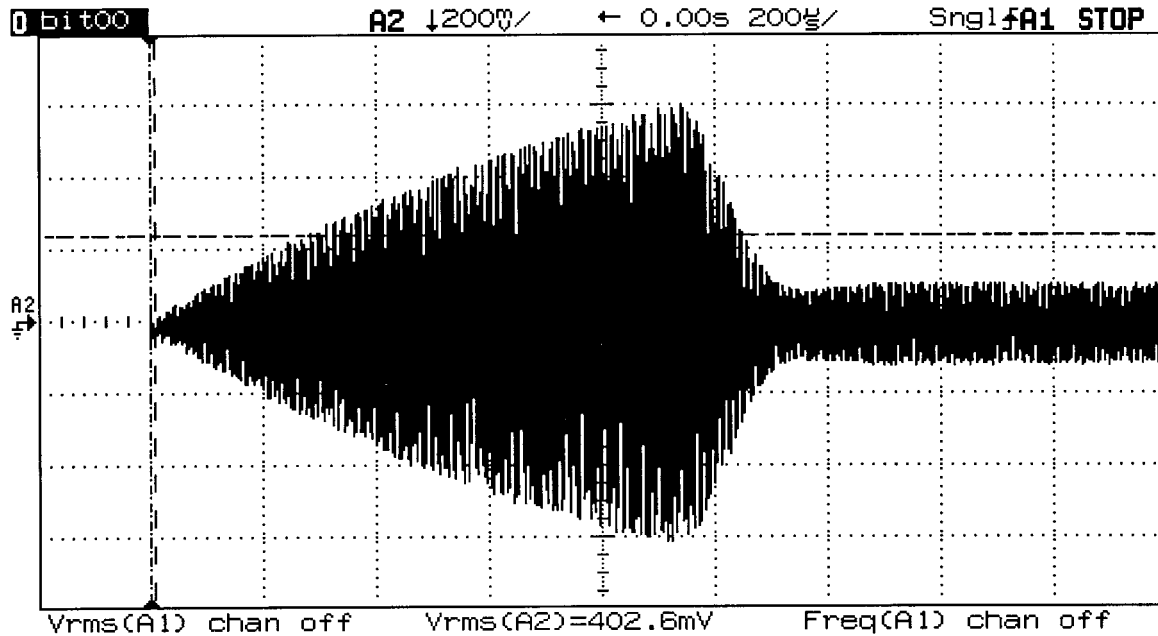
Figure 15: Current Waveform with Voltage = ±914 V
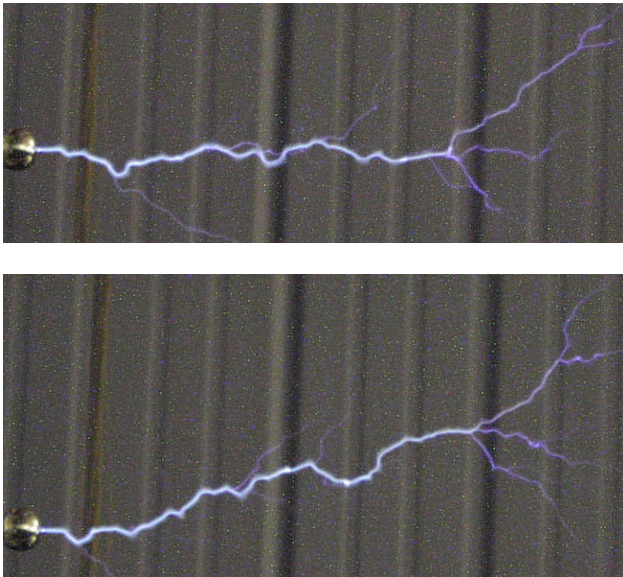


Figure 16: Onset plus 0.5 ms
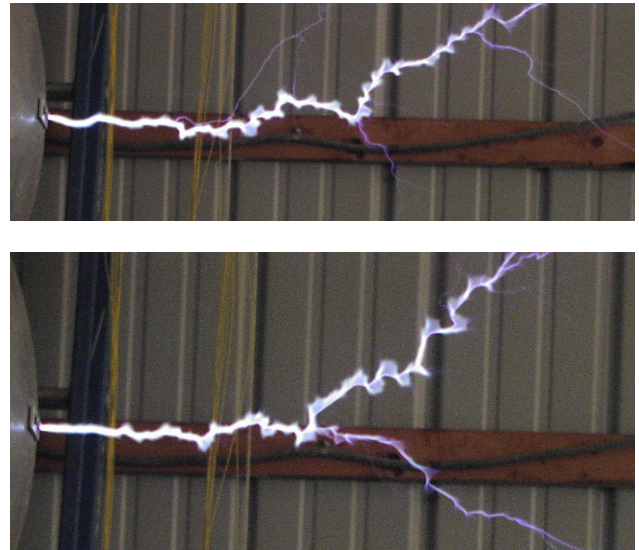


Figure 17: Onset plus 2 ms

[4] Cox, D. C., *Modern Resonance Transformer Design Theory*, Tesla Book Company, P. O. Box 1649, Greenville, TX 75401, (1984).

[5] Fawzi, Tharwat H. and P. E. Burke, *The Accurate Computation of Self and Mutual Inductances of Circular Coils*, IEEE Transactions on Power Apparatus and Systems, Vol. PAS-97, No. 2, March/April 1978, pp. 464-468.

[6] Fraga, E., C. Prados, and D.-X. Chen, "Practical Model and Calculation of AC Resistance of Long Solenoids", *IEEE Transactions on Magnetics*, Vol. 34, No. 1, January, 1998, pp. 205–212.

[7] Hull, Richard L., "The Tesla Coil Builder's Guide to The Colorado Springs Notes of Nikola Tesla",
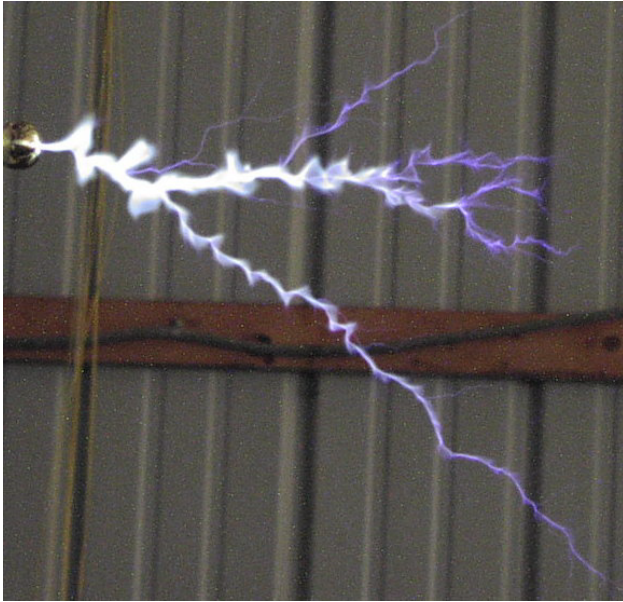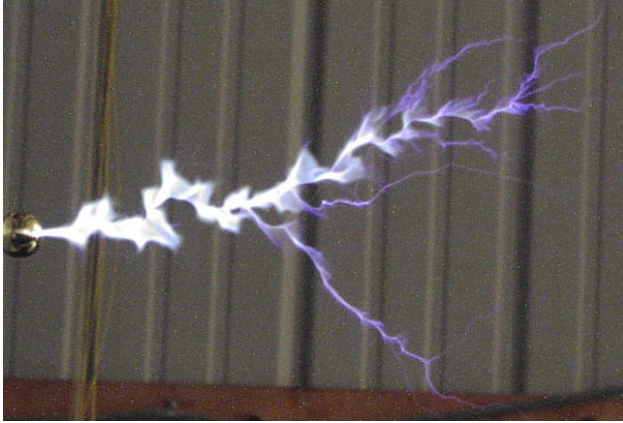
Figure 18: Onset plus 4 ms

Tesla Coil Builders of Richmond, 1993.

[8] Johnson, Gary L., "Using Power MOSFETs To Drive Resonant Transformers", *Tesla 88*, International Tesla Society, Inc., 330-A West Uintah, Suite 215, Colorado Springs, CO 80905, Vol. 4, No. 6, November/December 1988, pp. 7-13.

[9] Johnson, Gary L., *The Search For A New Energy Source*, Johnson Energy Corporation, P.O. Box 1032, Manhattan, KS 66505, 1997.

[10] Medhurst, R. G., "H.F. Resistance and Self-Capacitance of Single-Layer Solenoids", *Wireless Engineer*, February, 1947, pp. 35-43, and March, 1947, pp. 80-92.

[11] Peterson, Gary L., "Project Tesla Evaluated", *Power and Resonance, The International Tesla Society's Journal*, Volume 6, No. 1, January/February/ March 1990, pp. 25-34.

[12] Plonus, Martin A., *Applied Electromagnetics*, McGraw-Hill, New York, 1978.

[13] Schoessow, Michael, *TCBA News*, Vol. 6, No. 2, April/May/June 1987, pp. 12-15.

[14] Terman, Frederick Emmons, *Radio Engineers Handbook*, McGraw-Hill, 1943.

[15] Tesla, Nikola, *Colorado Springs Notes*, A. Marincic, Editor, Nolit, Beograd, Yugoslavia, 1978, 478 pages.